

# A tumor volume and performance status model to predict outcome before treatment in diffuse large B-cell lymphoma

Catherine Thieblemont,<sup>1</sup> Loic Chartier,<sup>2</sup> Ulrich Dührsen,<sup>3</sup> Umberto Vitolo,<sup>4</sup> Sally F. Barrington,<sup>5</sup> Jan M. Zaucha,<sup>6</sup> Laetitia Vercellino,<sup>7</sup> Maria Gomes Silva,<sup>8</sup> Ines Patrocinio-Carvalho,<sup>9</sup> Pierre Decazes,<sup>10</sup> Pierre-Julien Vially,<sup>11</sup> Herve Tilly,<sup>11</sup> Alina Berriolo-Riedinger,<sup>12</sup> Oliver Casasnovas,<sup>13</sup> Andreas Hüttmann,<sup>3</sup> Hajira Ilyas,<sup>5</sup> N. George Mikhaeel,<sup>14</sup> Joel Dunn,<sup>5</sup> Anne-Ségolène Cottreau,<sup>15</sup> Christine Schmitz,<sup>3</sup> Lale Kostakoglu,<sup>16</sup> Joseph N. Paulson,<sup>17</sup> Tina Nielsen,<sup>18</sup> and Michael Meignan<sup>19</sup>

<sup>1</sup>Hémato-oncologie, Université de Paris, Hôpital Saint-Louis, Assistance Publique-Hôpitaux de Paris (AP-HP), Paris, France; <sup>2</sup>Statistique, Lymphoma Academic Research Organisation, Pierre-Benite, France; <sup>3</sup>Hematology, Universitätsklinikum Essen, Essen, Germany; <sup>4</sup>Multidisciplinary Oncology Outpatient Clinic, Candiolo Cancer Institute, Fondazione del Piemonte per l'Oncologia Istituto di Ricovero e Cura a Carattere Scientifico, Candiolo, Italy; <sup>5</sup>King's College London & Guy's and St Thomas' PET Centre, School of Biomedical Engineering and Imaging Sciences, King's College London, London, United Kingdom; <sup>6</sup>Poland and Polish Lymphoma Research Group, Medical University of Gdańsk, Gdańsk, Poland; <sup>7</sup>Medecine Nucléaire, Hôpital Saint-Louis, AP-HP, Paris, France; <sup>8</sup>Hematology and <sup>9</sup>Nuclear Medecine, Instituto Português de Oncologia de Lisboa (IPO Lisboa), Lisbon, Portugal; <sup>10</sup>Medecine Nucléaire, Centre Henri Becquerel, Rouen, France; <sup>11</sup>Institut National de la Santé et de la Recherche Médicale U1245, Centre Henri Becquerel, Rouen, France; <sup>12</sup>Medecine Nucléaire, Centre Hospitalier Universitaire (CHU) le Bocage, Dijon, France; <sup>13</sup>Hématologie Centre, CHU le Bocage, Dijon, France; <sup>14</sup>Department of Clinical Oncology, Guy's & St Thomas' NHS Foundation Trust, School of Cancer & Pharmaceutical Sciences, King's College London, London, United Kingdom; <sup>15</sup>Medecine Nucléaire, Hôpital Cochin, AP-HP, Paris, France; <sup>16</sup>Radiology and Medical Imaging, University of Virginia, Charlottesville, VA; <sup>17</sup>Department of Biostatistics, Genentech Inc, South San Francisco, CA; <sup>18</sup>F. Hoffmann-La Roche Ltd, Basel, Switzerland; and <sup>19</sup>Lymphoma Study Association-Image Platform, Hôpital Henri Mondor, Créteil, France

## Key Points

- A new TMTV/ECOG-PS prognostic score was validated in 2174 patients of all ages with DLBCL treated in clinical trials and real-world series.
- The combined TMTV and ECOG-PS prognostic score allows identification of patients with high-risk DLBCL before first-line treatment.

Aggressive large B-cell lymphoma (LBCL) has variable outcomes. Current prognostic tools use factors for risk stratification that inadequately identify patients at high risk of refractory disease or relapse before initial treatment. A model associating 2 risk factors, total metabolic tumor volume (TMTV)  $>220 \text{ cm}^3$  (determined by fluorine-18 fluorodeoxyglucose positron emission tomography coupled with computed tomography) and performance status (PS)  $\geq 2$ , identified as prognostic in 301 older patients in the REMARC trial (#NCT01122472), was validated in 2174 patients of all ages treated in 2 clinical trials, PETAL (Positron Emission Tomography-Guided Therapy of Aggressive Non-Hodgkin Lymphomas; N = 510) and GOYA (N = 1315), and in real-world clinics (N = 349) across Europe and the United States. Three risk categories, low (no factors), intermediate (1 risk factor), and high (2 risk factors), significantly discriminated outcome in most of the series. Patients with 2 risk factors had worse outcomes than patients with no risk factors in the PETAL, GOYA, and real-world series. Patients with intermediate risk also had significantly worse outcomes than patients with no risk factors. The TMTV/Eastern Cooperative Oncology Group-PS combination outperformed the International Prognostic Index with a positive C-index for progression-free survival and overall survival in most series. The combination of high TMTV  $> 220 \text{ cm}^3$  and ECOG-PS  $\geq 2$  is a simple clinical model to identify aggressive LBCL risk categories before treatment. This combination addresses the unmet need to better predict before treatment initiation for aggressive LBCL the patients likely to benefit the most or not at all from therapy.

Submitted 27 December 2021; accepted 22 August 2022; prepublished online on *Blood Advances* First Edition 31 August 2022; final version published online 30 November 2022. <https://doi.org/10.1182/bloodadvances.2021006923>.

Data are available on request from the corresponding author, Catherine Thieblemont ([catherine.thieblemont@aphp.fr](mailto:catherine.thieblemont@aphp.fr)).

The full-text version of this article contains a data supplement.

© 2022 by The American Society of Hematology. Licensed under [Creative Commons Attribution-NonCommercial-NoDerivatives 4.0 International \(CC BY-NC-ND 4.0\)](https://creativecommons.org/licenses/by-nc-nd/4.0/), permitting only noncommercial, nonderivative use with attribution. All other rights reserved.

## Introduction

Aggressive large B-cell lymphoma (LBCL) is the most common subtype of non-Hodgkin lymphoma in adults, accounting for 30% to 40% of cases.<sup>1</sup> The heterogeneity of this disease has been recognized at the clinical, pathological,<sup>2,3</sup> and molecular levels,<sup>4-10</sup> leading to the identification of subtypes with different prognoses.<sup>1</sup> The aim of the initial therapy administered to patients with diffuse LBCL (DLBCL) is cure. Despite the complex heterogeneity of aggressive LBCL, rituximab plus cyclophosphamide, doxorubicin, vincristine, and prednisone (R-CHOP) has remained the standard therapy in previously untreated DLBCL for >15 years, achieving a cure in 60% of patients.<sup>11</sup> However, relapsing and refractory patients are reported in a large proportion of these patients, including 10% to 15% with primary refractory disease within 3 months after treatment and another 20% to 35% who relapse after initial efficacy.<sup>12,13</sup>

For the past 3 decades, tremendous efforts have been made to develop accessible and reproducible tools to identify relapsing and refractory patients early in the therapeutic management process. Developed in the early 1990s, the International Prognostic Index (IPI), is still widely used today. Validated in a cohort of 2031 patients of all ages, it incorporates 5 clinical parameters: age, serum lactate dehydrogenase (LDH) level, Eastern Cooperative Oncology Group performance status (ECOG-PS), disease stage, and number of extranodal sites.<sup>14</sup> The same clinical predictors were subsequently validated in the rituximab era (in the revised IPI [R-IPI]) in a real-world (RW) series of 365 patients.<sup>15</sup> More granular information about each of these 5 variables was included in the recent National Comprehensive Cancer Network IPI (NCCN-IPI) by analyzing outcomes from 1650 patients and validating the outcomes from 1138 patients.<sup>16</sup> The NCCN-IPI discriminates low- and high-risk subgroups (5-year overall survival [OS], 96% vs 33%, respectively) more effectively than the IPI (5-year OS, 90% vs 54%, respectively). However, these different IPI prognostic indices do not fully identify the relapsing and refractory patients. Attempts based on tumor biology are promising but not widely used.

Fluorine-18 fluorodeoxyglucose positron emission tomography coupled with computed tomography (PET-CT) is a highly precise functional imaging technique based on glucose avidity, which is recognized to be the most sensitive imaging modality for staging DLBCL.<sup>17-21</sup> The routine implementation of this technique has improved the prognostic value of the IPI and R-IPI.<sup>22,23</sup> More recently, PET-CT studies have suggested that the baseline total metabolic tumor volume (TMTV), that is, the sum of the metabolic volume of all lesions, is an accurate quantification of tumor burden and a strong prognostic indicator of outcome in DLBCL and several lymphoma subtypes.<sup>24-29</sup> Compared with molecular heterogeneity, TMTV improves the risk stratification in DLBCL.<sup>28-30</sup> TMTV measures tumor burden and partially replaces several IPI parameters that are surrogates of the tumor burden (LDH, stage, and extranodal site).

We recently reported results of a study in 301 older patients with aggressive LBCL responding to first-line R-CHOP in the phase 3 REMARC study, showing the strong prognostic value of the combination of baseline high TMTV (>220 cm<sup>3</sup>) and worse ECOG-PS ( $\geq 2$ ), to identify, before receiving treatment, the refractory/relapsed

population aged 60 to 80 years, that was not identified by IPI or NCCN-IPI (supplemental Figure 1).<sup>29</sup> This new score derives from the IPI by combining TMTV and another parameter of the IPI, that is, the ECOG-PS characterizing the patient status. Extending the strong prognostic impact of this simple combination to other risk categories of patients with DLBCL would render it a broadly applicable, important new tool for detecting refractory/relapsed patients, before the initiation of first-line treatment, thereby allowing treating physicians to offer their patients innovative therapeutic strategies.

We applied this combined TMTV and ECOG-PS score to a large adult patient population with aggressive LBCL covering all age groups, including 2174 patients with DLBCL identified from multiple international cohorts, to cover the most common clinical settings since the introduction of PET in lymphoma management. Patients from 2 large prospective randomized trials (with one trial including a PET response to treatment-guided strategy) as well as an RW series of patients (who were not treated in clinical trials), were analyzed using the combined TMTV and ECOG-PS score determined using the REMARC study.<sup>29</sup> This validation approach allowed the inclusion of patients with variable response to standard first-line treatment and without selection bias. The goal of the study was to validate the prognostic factor model for its broad application in aggressive LBCL.

## Methods

### Study design and data collection

Clinical data were collected from 2174 patients with aggressive LBCL treated in 2 randomized clinical trials in Europe and the United States, GOYA (N = 1315) and PETAL (Positron Emission Tomography-Guided Therapy of Aggressive Non-Hodgkin Lymphomas; N = 510), and patients treated in RW (N = 349) clinics across multiple European centers (supplemental Table 1 provides a brief description). The study database included data to assess progression-free survival (PFS), OS, and the dichotomized parameters that contribute to the IPI. Associations of TMTV and ECOG-PS at baseline were explored according to the IPI and survival outcomes. Patients participating in the 2 clinical trials and patients receiving treatment in RW clinics provided written informed consent for use of their data, and all contributing studies were approved by the institutional review boards.

### Baseline TMTV

Anonymized baseline PET-CT images were collected. TMTV measurements were performed by experienced nuclear medicine physicians (L.V., A.-S.C., M.M., U.D., C.S., S.F.B., I.P.-C., L.K.) blinded to patient outcomes.

TMTV was computed using either the 41% maximum standardized uptake value (SUV<sub>max</sub>) threshold method, as published for various lymphoma subtypes,<sup>25,26,28,29,31-33</sup> or with a systematic subtraction of the SUV<sub>max</sub> of the liver multiplied by 1.5 (GOYA study).<sup>30</sup> Semiautomated software was used, including Hermes<sup>24</sup> and Beth Israel Fiji20 ([www.petctviewer.org](http://www.petctviewer.org)) for the RW series (as used in the REMARC study),<sup>29</sup> Medical Image Merge for the GOYA trial,<sup>30</sup> and Accurate (<https://petralymphoma.org>) for the PETAL trial.<sup>27</sup> The TMTV in the GOYA trial was computed using a method that differed from the 41% SUV<sub>max</sub> threshold method

used in the PETAL trial, RW series, and REMARC study. To ensure the consistency of the results between the series despite different initial TMTV measurements, the distribution of TMTV values of GOYA was realigned on the TMTV REMARC distribution using the combating batch effect method<sup>34</sup> (described in the supplemental Data for calibration methodology).

## Statistical analysis

PFS was defined according to the revised response criteria for malignant lymphomas.<sup>21</sup> Survival functions were calculated by Kaplan-Meier estimates, and confidence intervals were calculated using Greenwood approximation.<sup>35</sup> The Cox proportional hazards model was used for the estimation of hazard ratio and its confidence interval, using the low-risk group as the reference.

The combination of high TMTV ( $>220\text{ cm}^3$ ) and worse ECOG-PS ( $\geq 2$ ) was previously defined in a training set from the REMARC study.<sup>29</sup> Patients from GOYA, PETAL, and RW constituted the validation set of the initial REMARC training population. The discriminatory power of the TMTV/ECOG-PS model was compared with that of the IPI using net reclassification improvement (NRI)<sup>36</sup> and C-index calculations. The category-free NRI and the 3-category index ( $\text{NRI}^{0.2,0.4}$ ) with a cutoff at 0.20 and 0.40 defining low-, medium-, and high-risk categories were calculated to ensure the robustness of conclusion. A *P* value of  $\leq 0.05$  was considered statistically significant. Statistical analyses were performed using SAS version 9.3 and R version 3.6.2.

## Results

### Characterization of the GOYA, PETAL, and RW series

Clinical characteristics of the 2174 patients included in PETAL ( $N = 510$ ), GOYA ( $N = 1315$ ), and the RW series ( $N = 349$ ) are summarized in Table 1. More than half of the patients were classified as IPI 0 to 2 (55%) and age-adjusted IPI (aaIPI) 0 to 1 (52%) and had  $\text{TMTV} > 220\text{ cm}^3$  (55%). The 3 cohorts differed in median follow-up duration, selected clinical characteristics, and tumor burden. Percentages of patients aged  $\geq 60$  years, ECOG-PS  $\geq 2$ , elevated LDH level, aaIPI 2 to 3, and IPI 3 to 5 were higher in the RW series than in the PETAL and GOYA trials. In GOYA, median TMTV and percentage of patients with  $\text{TMTV} > 220\text{ cm}^3$  were higher than in the PETAL and RW series. The percentage of patients with  $\text{TMTV} \leq 220\text{ cm}^3$  and ECOG-PS  $< 2$  (no factors) was lower, and the percentage of patients with only 1 risk factor (either  $\text{TMTV} > 220\text{ cm}^3$  or ECOG-PS  $\geq 2$ ) was higher in the GOYA cohort than in the PETAL and RW cohorts. The 2 risk factors ( $\text{TMTV} > 220\text{ cm}^3$  and ECOG-PS  $\geq 2$ ) were reported in a higher proportion of the RW series than in the GOYA or PETAL series. Differences were also seen in terms of clinical outcomes; the rate of PFS events was higher in the RW series (41.8%) than in the PETAL and GOYA trials (30.2% and 31.4%, respectively), as was the rate of OS events (35.8% vs 21.2% and 20.1%, respectively).

### Prognostic value of ECOG-PS, TMTV, and IPI

ECOG-PS, TMTV, and IPI were prognostic in all 3 series. The factors ECOG-PS  $\geq 2$ ,  $\text{TMTV} > 220\text{ cm}^3$ , and IPI 3 to 5 discriminated subgroups of patients with significantly different prognoses for PFS and OS, as reported in Tables 2 and 3. This was confirmed in the analysis of the hazard ratio of ECOG-PS 0 to 1 vs ECOG-PS

$\geq 2$ ,  $\text{TMTV} > 220\text{ cm}^3$  vs  $\text{TMTV} \leq 220\text{ cm}^3$ , and IPI 3 to 5 vs IPI 0 to 2 (Tables 2 and 3).

### Combined TMTV/ECOG-PS and IPI

The TMTV/ECOG-PS score stratifies patients in all studies into 3 different risk groups. Four-year PFS and OS decreased (Figure 1A; Tables 2 and 3) from the low-risk group with no risk factors ( $\text{TMTV} \leq 220\text{ cm}^3$ , ECOG-PS  $< 2$ ) to the intermediate-risk group with 1 adverse factor ( $\text{TMTV} > 220\text{ cm}^3$  or ECOG-PS  $\geq 2$ ). The lowest PFS and OS were observed in the high-risk group with 2 risk factors ( $\text{TMTV} > 220\text{ cm}^3$  and ECOG-PS  $\geq 2$ ). We performed a comparison between the classification of patients in the high-risk category using the TMTV/ECOG-PS score or the IPI score (IPI 3-5). Kaplan-Meier survival curves considering risk groups (IPI 0-1, IPI 2, IPI 3, and IPI 4-5) based on the IPI are shown in supplemental Figure 2. In the PETAL, GOYA, and RW series, 47 of 510 (9%), 130 of 1315 (10%), and 62 of 349 (18%) patients, respectively, were identified as high risk, according to the combined TMTV/ECOG-PS, vs 195 of 510 (38.3%), 579 of 1315 (44%), and 207 of 349 (59.3%) patients with an IPI score of 3 to 5. The combined TMTV/ECOG-PS allowed better identification of patients with shorter PFS and OS than did the IPI (Figure 1B; Table 3). The combined TMTV/ECOG-PS model displayed higher model performance than IPI in most of the series, showing (1) a higher C-index for both PFS and OS observed in the RW and PETAL series (Table 4); and (2) a higher category-free NRI index for PFS, mainly owing to  $\text{NRI}_{\text{ne}}$  (from +48.1% to +56.5% in PETAL, from -7.0% to +12.3% in GOYA, and from +25.0% to +60.0% in RW series), suggesting that the TMTV/ECOG-PS score improves prediction for nonevents. The same trend was observed in the PETAL trial for OS with a  $\text{NRI}_{\text{ne}}$  from +43.1% to +55.0% but not in GOYA where higher NRI is mainly owing to  $\text{NRI}_{\text{e}}$  (from +8.9% to +20.3%). No trend either in favor of  $\text{NRI}_{\text{ne}}$  or in favor of  $\text{NRI}_{\text{e}}$  was observed in the RW series for OS (Table 4). The same conclusion was observed with the 3-category index (data not shown).

### Stratification by age $< 60$ vs $\geq 60$ years

We further examined the performance of the predictive value of the combined TMTV/ECOG-PS model in subgroups of patients using the age threshold of 60 years. Patient characteristics in these subgroups are described in supplemental Table 2. The percentage of patients with 2 risk factors ( $\text{TMTV} > 220\text{ cm}^3$  and ECOG-PS  $\geq 2$ ) was higher in the RW series than in the PETAL and GOYA trials for patients aged  $< 60$  years and for patients aged  $\geq 60$  years. PFS and OS are displayed for patients according to the 60-year age threshold in supplemental Figures 3 and 4. In all 3 studies, the combined TMTV/ECOG-PS displayed high model performance, except for patients aged  $< 60$  years in the GOYA study (Table 4).

## Discussion

This study validates in 2174 patients with aggressive LBCL across multiple international cohorts, the prognostic impact of the combination of the metabolic tumor volume from baseline PET-CT scans and a simple, routine clinical evaluation, ECOG-PS, which was first described in 301 older patients with aggressive LBCL who presented with a chemosensitive lymphoma to first-line treatment.<sup>29</sup> Our validation cohort was derived from 2 large global prospective randomized clinical trials (one of which was a

**Table 1. Clinical characteristics of patients included in the 3 clinical series used to validate the TMTV/ECOG-PS model**

Characteristics	PETAL (N = 510)	GOYA (N = 1315)	RW series (N = 349)
Median age, y, n (range)	62 (18-80)	62 (18-86)	66 (17-92)
Age ≥60 y, n (%)	280 (54.9)	758 (57.6)	255 (73.1)
<b>Sex</b>			
Male, n (%)	279 (54.7)	698 (53.1)	169 (48.4)
Female, n (%)	231 (45.3)	617 (46.9)	180 (51.6)
<b>Histology</b>			
DLBCL not otherwise specified, n (%)	479 (93.9)	1186 (90.2)	186 (92.1)
FL grade 3B, n (%)	14 (2.7)	0 (0)	0 (0)
De novo transformed, n (%)	17 (3.3)	0 (0)	10 (5.0)
Other, n (%)	0 (0)	129 (9.8)	6 (3.0)
Missing, n	0	0	147
<b>ECOG-PS</b>			
0–1, n (%)	451 (89.1)	1152 (87.6)	259 (74.2)
≥2, n (%)	55 (10.9)	163 (12.4)	90 (25.8)
Missing, n	4	0	0
<b>Ann Arbor stage</b>			
I-II, n (%)	214 (42.0)	314 (23.9)	93 (26.7)
III-IV, n (%)	295 (58.0)	1001 (76.1)	256 (73.3)
Missing, n	1	0	0
<b>Extranodal sites</b>			
<2, n (%)	350 (68.8)	854 (64.9)	210 (62.3)
>2, n (%)	159 (31.2)	461 (35.1)	127 (37.7)
Missing, n	1	0	12
<b>Elevated LDH (&gt;upper limit of normal)</b>			
No, n (%)	222 (43.6)	558 (42.6)	130 (37.4)
Yes, n (%)	287 (56.4)	753 (57.4)	218 (62.6)
Missing, n (%)	1	4	1
<b>Age-adjusted IPI</b>			
0-1, n (%)	290 (57.1)	686 (52.2)	146 (41.8)
2-3, n (%)	218 (42.9)	629 (47.8)	203 (58.2)
Missing, n	2	0	0
<b>IPI</b>			
0-2, n (%)	314 (61.7)	736 (56.0)	142 (40.7)
3-5, n (%)	195 (38.3)	579 (44.0)	207 (59.3)
Missing, n	1	0	0
<b>Treatment</b>			
R-CHOP, n (%)	486 (95.3)	654 (49.7)	
G-CHOP, n (%)	–	661 (50.3)	349 (100)
Intensified CHOP/CHOP, n (%)	24 (4.7)	–	–
<b>TMTV (cm<sup>3</sup>)</b>			
Median, n (range)	177 (1-8896)	269 (2-8113)	188 (0-3764)
TMTV >220 cm <sup>3</sup> , n (%)	231 (45.3)	725 (55.1)	157 (45.0)

Number of patients (%) presented unless otherwise specified.

G-CHOP, obinutuzumab CHOP.

\*Risk factors are TMTV >220 cm<sup>3</sup> and ECOG-PS ≥2.

PET-guided trial) and a RW series of patients treated across multiple European centers. This combination of simple, accessible, and highly reproducible imaging and clinical parameters allows us to identify before treatment the patients at the lowest risk and those

who are at high risk of treatment failure and death before receiving the first dose of first-line standard or intensified immunochemotherapy. This novel TMTV/ECOG-PS tool enabled the prediction of patients likely or unlikely to benefit from the treatment. The small



**Table 1 (continued)**

Characteristics	PETAL (N = 510)	GOYA (N = 1315)	RW series (N = 349)
<b>Combined TMTV and ECOG-PS risk factors*</b>			
0 factor, n (%)	270 (53.0)	553 (42.1)	164 (47.0)
1 factor, n (%)	192 (37.7)	636 (48.4)	123 (35.2)
2 factors, n (%)	47 (9.2)	126 (9.6)	62 (17.8)
Missing, n	1		
Median follow-up, mo	54.7	47.1	76.5

Number of patients (%) presented unless otherwise specified.

G-CHOP, obinutuzumab CHOP.

\*Risk factors are TMTV >220 cm<sup>3</sup> and ECOG-PS ≥2.

high-risk set of patients identified by the TMTV/ECOG-PS tool represents in our study ~10% to 20% of patients with aggressive LBCL. This is in the order of magnitude of the percentage of patients with poor prognosis, including patients with a lymphoma refractory to R-CHOP<sup>11,12</sup> or patients who initially responded to R-CHOP but who subsequently relapsed.<sup>29</sup>

In the 27 years since the publication of the IPI, this index has been refined numerous times to account for the evolving treatment landscape, including the widely implemented R-IPI and the recent NCCN-IPI.<sup>37</sup> These indices use standard clinical and laboratory factors to predict outcome. Other clinical factors, such as tumor size, have also been correlated with outcome; however, the definition of “bulky disease” varies among studies, ranging from 5 to 10 cm.<sup>38</sup> In our study, baseline tumor burden was assessed using TMTV by different investigators, methods, and software across Europe and North America,<sup>39</sup> within large and heterogeneous patient populations. Importantly, we confirmed that measurement of TMTV is feasible in this setting and is prognostic of outcome irrespective of the method used, including free online or commercialized software, thus representing a widely accessible tool. TMTV more accurately quantifies tumor burden for determining prognosis than the diameter of the largest lesion. It has been shown in DLBCL that there is a continuous increase of risk for PFS and OS with increasing TMTV. In the GOYA study, the number of events increased with TMTV quartiles.<sup>30</sup> For this reason, our threshold of 220 cm<sup>3</sup> could be applied successfully in the GOYA study despite differences in TMTV measurement. Furthermore, the results of the combating match effect method, which calibrates TMTV measurements to a given reference, the TMTV GOYA calibrated measures, confirms the validity of this cutoff. In this analysis, the distribution of the TMTV values in the REMARC study was used as a reference. After this transformation, the 2 distributions can be safely compared despite the different methods of TMTV measurement. We have demonstrated that the TMTV threshold of 220 cm<sup>3</sup> combined with ECOG-PS is a sensitive tool to detect not only the high-risk groups among responders to R-CHOP who were included in the REMARC study but also these high-risk groups in a large population of patients with different levels of risk. This was true in the clinical settings of both experimental clinical trials with selected patients and in the RW sample. Interestingly, the clinical characteristics of the cohorts of patients among these 3 series were not identical, with more patients with ECOG-PS 0 to 1 in the PETAL and GOYA series than in the RW series, and a lower percentage of patients with disseminated disease, elevated

disease, and IPI 4 to 5 in the PETAL series than in the GOYA and RW series. However, the discrimination based on the TMTV/ECOG-PS score was maintained.

We also validated the tool in subsets of patients using the 60-year age threshold. This stratification has been used historically, notably with the specific aalPI developed for patients aged <60 years. The aalPI is routinely used in clinical practice and trials in which more intensive experimental approaches are tested in younger patients. In both age-based subgroups, the combination TMTV/ECOG-PS was more powerful for predicting high-risk patients than the IPI, highlighting the robustness of the TMTV/ECOG-PS combination, and could be used to further refine available prognostic factor models for aggressive LBCL.

In this validation analysis, we identified those patients with low, intermediate, and high risk of poor outcome based on a single imaging and a single clinical estimate before treatment initiation, reflecting the ease and feasibility of its implementation in the routine clinical setting. These parameters represent only a small aspect of the heterogeneity that exists in aggressive LBCL, such as the spread of the lesions measured by distance between lesions, as previously reported.<sup>40</sup> Furthermore, estimation of tumor burden based on circulating tumor DNA (ctDNA) is emerging as a non-imaging biomarker in B-cell lymphoma to capture and monitor refractory disease. Pretreatment ctDNA levels have been shown to reflect tumor burden and to predict treatment outcomes.<sup>41</sup> Together, radiomics, of which TMTV is the main feature on which most of the other features depend, clinical parameters, lymphoma biology, ctDNA, genomics, and minimal residual disease are likely to play an increasingly prominent role in selecting patients for specific therapies in future investigations and to refine the current index to achieve a risk-tailored therapy.<sup>42</sup> To exploit and translate these results into clinical practice, we need to continue moving toward standardization of these tools. This study with data from prospective trials and RW scenarios contributes to this standardization. The goal of treatment would then be anticipatory; patients at low risk may be treated with conventional approaches, unless an appropriate clinical trial is available. This will avoid exposing them to unnecessary treatment. Within intermediate- and high-risk groups, patients will be encouraged to enroll in studies exploring the efficacy of novel regimens directed at specific targets suggested by genetic and molecular subtyping, with some specific agents already available (eg, tazemetostat, Bruton tyrosine kinase inhibitors, venetoclax, upfront chimeric antigen receptor T cells, or bispecific T-cell engager antibodies).<sup>42</sup>

**Table 2. Impact of TMTV, ECOG-PS, IPI, and combined TMTV/ECOG-PS for survival (PFS and OS) in the PETAL, GOYA, and RW series**

Variables and index	PETAL, HR (95% CI), P value		GOYA, HR (95% CI), P value		RW, HR (95% CI), P value	
	PFS	OS	PFS	OS	PFS	OS
ECOG-PS $\geq 2$	1.94 (1.30-3.00), .006	2.46 (1.50-4.00), <.001	1.75 (1.37-2.22), <.001	1.95 (1.47-2.59), <.001	2.18 (1.50-3.10), <.001	2.61 (1.80-3.80), <.001
TMTV >220 cm <sup>3</sup>	2.88 (2.10-4.00), <.001	2.69 (1.80-4.00), <.001	1.75 (1.43-2.14), <.001	1.84 (1.42-2.38), <.001	2.73 (1.90-3.80), <.001	2.80 (1.90-4.10), <.001
IPI 3-5	2.33 (1.70-3.20), <.001	2.41 (1.70-3.50), <.001	1.81 (1.50-2.2), <.001	2.1 (1.70-2.60), <.001	2.42 (1.70-3.50), <.001	3.23 (2.10-5.00), <.001
<b>Combined TMTV/ECOG-PS*</b>						
1 risk factor	2.92 (2.00-4.20), <.001	2.71 (1.80-4.20), <.001	1.47 (1.18-1.82), .00493	1.46 (1.11-1.92), .00683	2.37 (1.60-3.50), <.001	2.24 (1.40-3.50), <.001
2 risk factors	3.32 (2.00-5.50), <.001	3.85 (2.20-6.80), <.001	2.85 (2.11-3.84), <.001	3.35 (2.34-4.78), <.001	3.85 (2.50-5.90), <.001	4.61 (2.90-7.30), <.001

CI, confidence interval; HR, hazard ratio.

\*Risk factors are TMTV >220 cm<sup>3</sup> and ECOG-PS  $\geq 2$ .**Table 3. Four-year PFS and OS according to prognostic scoring systems in the PETAL, GOYA, and RW series**

Scores	PETAL		GOYA		RW	
	4-y PFS, % (95% CI)	4-y OS, % (95% CI)	4-y PFS, % (95% CI)	4-y OS, % (95% CI)	4-y PFS, % (95% CI)	4-y OS, % (95% CI)
TMTV/ECOG-PS high risk*	54 (39-67)	61 (45-73)	49 (40-59)	61 (52-70)	36 (24-48)	41 (28-53)
IPI 3-5	59 (52-66)	70 (63-76)	58 (54-62)	72 (69-76)	55 (48-62)	59 (52-65)
TMTV/ECOG-PS intermediate risk†	57 (50-64)	72 (65-79)	65 (61-69)	80 (76-83)	57 (47-65)	64 (54-72)
IPI 0-2	79 (73-83)	86 (82-90)	73 (70-76)	85 (83-88)	75 (67-81)	84 (77-89)
TMTV/ECOG-PS low risk	84 (79-88)	90 (85-93)	73 (69-77)	85 (82-89)	78 (71-83)	84 (77-89)

\*Two risk factors, ECOG-PS  $\geq 2$  and TMTV >220 cm<sup>3</sup>.†One risk factor, ECOG-PS  $\geq 2$  and TMTV  $\leq 220$  cm<sup>3</sup> or ECOG-PS <2 and TMTV >220 cm<sup>3</sup>.

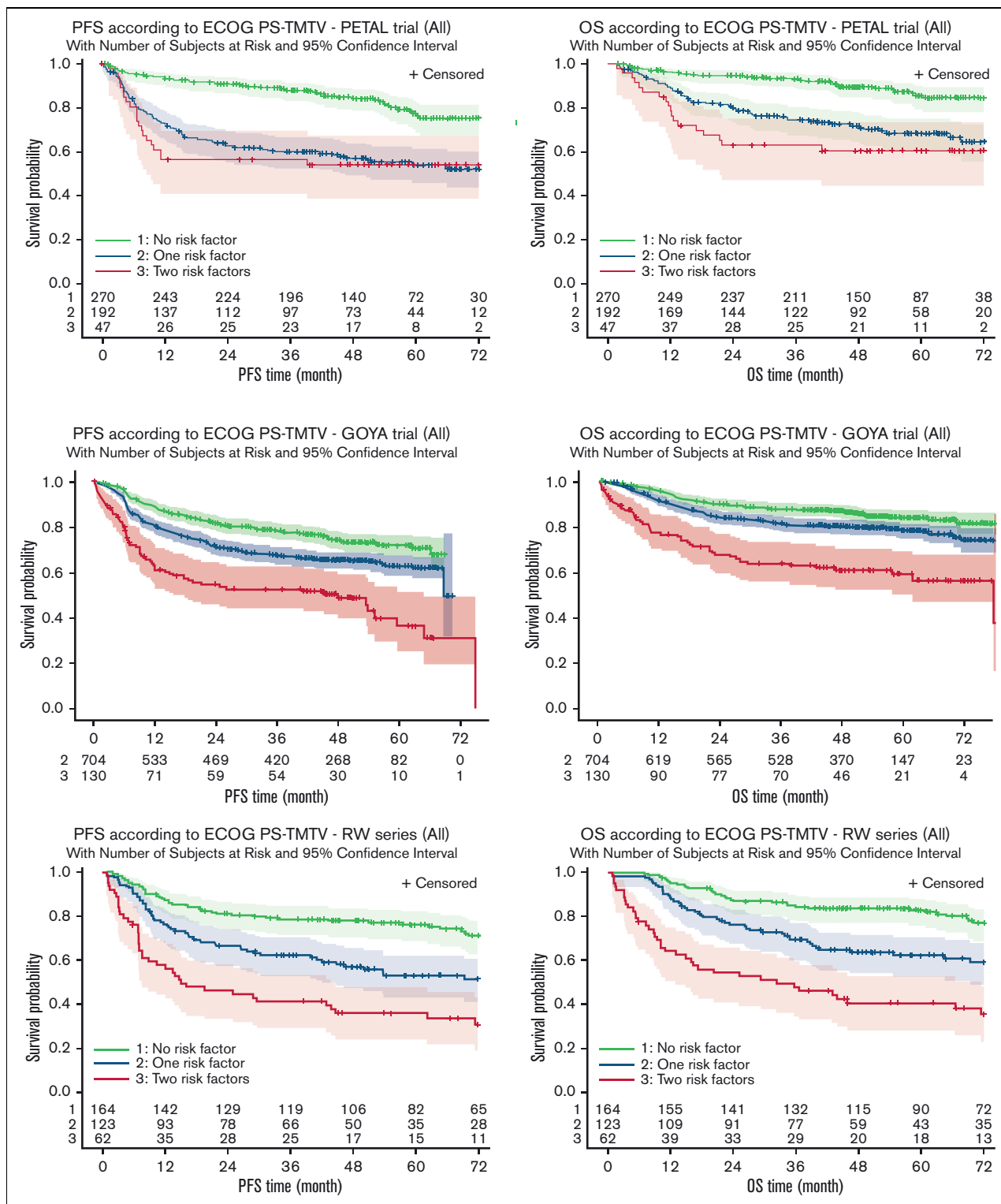


**Figure 1. Kaplan-Meier estimates of survival (PFS and OS) according to risk groups.** (A-F) Estimates are based on the risk factors TMTV >220 cm<sup>3</sup> and ECOG-PS ≥2 in the PETAL (A,B), GOYA (C,D), and RW (E,F) series.

**Table 4. Comparison of the combined TMTV/ECOG-PS with IPI in high-risk patients**

Indexes	PETAL		GOYA		RW	
	PFS	OS	PFS	OS	PFS	OS
All patients (N = 2174)						
NRI (±SE)	+0.21 (0.09)	+0.24 (0.10)	+0.24 (0.07)	+0.15 (0.056)	0.00 (0.10)	-0.17 (0.11)
NRI <sub>e</sub> /NRI <sub>he</sub> , %	-35.1/+56.5	-31.5/+55.0	-9.9/+12.3	+8.9/+6.5	-28.8/+29.1	-0.8/-16.1
C-index (difference vs IPI)	0.655 (+0.046)	0.658 (+0.039)	0.6065 (-0.0379)	0.6237 (-0.0367)	0.643 (+0.048)	0.666 (+0.043)
<60 y (n = 884)						
NRI (±SE)	+0.54 (0.15)	+0.66 (0.19)	+0.041 (0.08)	+0.14 (0.06)	+0.48 (0.20)	+0.06 (0.23)
NRI <sub>e</sub> /NRI <sub>he</sub> , %	+5.1/+48.5	+22.6/+43.1	+1.1/+3.1	+20.3/-5.9	-11.8/+60.0	+21.7/-15.5
C-index (difference vs IPI)	0.687 (+0.091)	0.695 (+ 0.096)	0.6199 (-0.0387)	0.6495 (-0.0327)	0.600 (+0.022)	0.619 (+0.008)
>60 y (n = 1293)						
NRI (±SE)	+0.54 (0.12)	+0.55 (0.13)	+0.07 (0.07)	+0.13 (0.07)	+0.03 (0.13)	+0.01 (0.13)
NRI <sub>e</sub> /NRI <sub>he</sub> , %	+6.4/+48.1	+10.5/+44.8	+14.3/-7.0	+12.3/+1.1	-22.4/+25.0	-4.4/+5.4
C-index (difference vs IPI)	0.633 (+0.030)	0.640 (+ 0.045)	0.5994 (-0.0457)	0.6074 (-0.0521)	0.654 (+0.068)	0.665 (+0.068)

NRI<sub>e</sub>, event NRI; NRI<sub>he</sub>, nonevent NRI; SE, standard error.

In conclusion, despite the marked heterogeneity of aggressive LBCL, we have demonstrated that the combination of TMTV and ECOG-PS is a reliable tool that may be used in complement to IPI with important clinical implications for upfront identification of those patients with aggressive LBCL who can feasibly be enrolled in studies exploring the efficacy of novel regimens directed at specific targets.

### Acknowledgments

The authors thank the patients and their families enrolled in the 3 series of this analysis and Sarah MacKenzie for editorial assistance.

### Authorship

Contribution: C.T., L.C., and M.M. conceived and designed the study; C.T., L.C., J.N.P., and M.M. wrote the manuscript; and all authors provided study material or patients, collected, and assembled data, performed data analysis and interpretation, provided final approval of the manuscript, and are accountable for all aspects of the work.

Conflict-of-interest disclosure: C.T. received honoraria from Roche, Amgen, Janssen, Celgene, and Gilead Science/Kyte; has been in a consulting/advisory role for Roche, Gilead Sciences, Janssen, Celgene, and Novartis; and has received research funding and travel, accommodations, and expenses from Roche and Novartis. U.D. provided consultation to AbbVie, Amgen, CPT, Gilead/Kite, Janssen, Novartis, and Takeda; has received research funding from Amgen, Celgene, and Roche; and has received

honoraria from AbbVie, Alexion, Amgen, Celgene, CPT, Gilead/Kite, Janssen, Novartis, Roche, and Takeda. U.V. has received honoraria from Roche and Janssen. J.M.Z. provided consultation to Novartis, Bristol Myers Squibb, Takeda, Roche, and Sandoz; and received honoraria from Takeda, Roche, AbbVie, and Sandoz. M.G.S. provided consultation to Roche, AbbVie, Bristol Myers Squibb, Merck Sharp & Dohme, Janssen, and Gilead; has received research funding from Gilead Sciences; and has received honoraria from Roche, Janssen, Gilead, and AbbVie. O.C. has provided consultation to Roche, Takeda, Gilead, AbbVie, Merck Sharp & Dohme, and Amgen; has received research funding from Roche, Gilead, and Takeda; and has received honoraria from Roche, Takeda, Gilead, AbbVie, Merck Sharp & Dohme, and Amgen. A.H. has received honoraria from Celgene, Gilead, and Takeda. M.M. has provided consultation to and received honoraria from Roche. The remaining authors declare no competing financial interests.

ORCID profiles: C.T., [0000-0002-9941-2448](https://orcid.org/0000-0002-9941-2448); U.V., [0000-0001-7772-2747](https://orcid.org/0000-0001-7772-2747); S.F.B., [0000-0002-2516-5288](https://orcid.org/0000-0002-2516-5288); M.G.S., [0000-0002-6993-2450](https://orcid.org/0000-0002-6993-2450); I.P.-C., [0000-0003-2523-4754](https://orcid.org/0000-0003-2523-4754); P.D., [0000-0001-5323-9910](https://orcid.org/0000-0001-5323-9910); A.B.-R., [0000-0003-0771-7824](https://orcid.org/0000-0003-0771-7824); O.C., [0000-0002-1156-8983](https://orcid.org/0000-0002-1156-8983); A.H., [0000-0003-2230-3873](https://orcid.org/0000-0003-2230-3873); N.G.M., [0000-0003-0359-0328](https://orcid.org/0000-0003-0359-0328).

Correspondence: Catherine Thieblemont, Hemato-oncologie, Hôpital Saint-Louis, Assistance Publique-Hôpitaux de Paris, 1 Avenue Claude Vellefaux, Paris 75010, France; email: [catherine.thieblemont@aphp.fr](mailto:catherine.thieblemont@aphp.fr).

### References

1. Swerdlow SH, Campo E, Pileri SA, et al. The 2016 revision of the World Health Organization classification of lymphoid neoplasms. *Blood*. 2016;127(20):2375-2390.
2. Hans CP, Weisenburger DD, Greiner TC, et al. Confirmation of the molecular classification of diffuse large B-cell lymphoma by immunohistochemistry using a tissue microarray. *Blood*. 2004;103(1):275-282.
3. Scott DW, King RL, Staiger AM, et al. High-grade B-cell lymphoma with MYC and BCL2 and/or BCL6 rearrangements with diffuse large B-cell lymphoma morphology. *Blood*. 2018;131(18):2060-2064.



4. Alizadeh AA, Eisen MB, Davis RE, et al. Distinct types of diffuse large B-cell lymphoma identified by gene expression profiling. *Nature*. 2000;403(6769):503-511.
5. Lenz G, Davis RE, Ngo VN, et al. Oncogenic CARD11 mutations in human diffuse large B cell lymphoma. *Science*. 2008;319(5870):1676-1679.
6. Hu S, Xu-Monette ZY, Tzankov A, et al. MYC/BCL2 protein coexpression contributes to the inferior survival of activated B-cell subtype of diffuse large B-cell lymphoma and demonstrates high-risk gene expression signatures: a report from The International DLBCL Rituximab-CHOP Consortium Program. *Blood*. 2013;121(20):4021-4250.
7. Chapuy B, Stewart C, Dunford AJ, et al. Molecular subtypes of diffuse large B cell lymphoma are associated with distinct pathogenic mechanisms and outcomes. *Nat Med*. 2018;24(5):679-690.
8. Schmitz R, Wright GW, Huang DW, et al. Genetics and pathogenesis of diffuse large B-cell lymphoma. *N Engl J Med*. 2018;378(15):1396-1407.
9. Wright GW, Huang DW, Phelan JD, et al. A probabilistic classification tool for genetic subtypes of diffuse large B cell lymphoma with therapeutic implications. *Cancer Cell*. 2020;37(4):551-568.e14.
10. Reddy A, Zhang J, Davis NS, et al. Genetic and functional drivers of diffuse large B cell lymphoma. *Cell*. 2017;171(2):481-494.e15.
11. Coiffier B, Thieblemont C, Van Den Neste E, et al. Long-term outcome of patients in the LNH-98.5 trial, the first randomized study comparing rituximab-CHOP to standard CHOP chemotherapy in DLBCL patients: a study by the Groupe d'Etudes des Lymphomes de l'Adulte. *Blood*. 2010;116(12):2040-2045.
12. Sehn LH, Gascoyne RD. Diffuse large B-cell lymphoma: optimizing outcome in the context of clinical and biologic heterogeneity. *Blood*. 2015;125(1):22-32.
13. Thieblemont C, Tilly H, Gomes da Silva M, et al. Lenalidomide maintenance compared with placebo in responding elderly patients with diffuse large B-cell lymphoma treated with first-line rituximab plus cyclophosphamide, doxorubicin, vincristine, and prednisone. *J Clin Oncol*. 2017;35(22):2473-2481.
14. International Non-Hodgkin's Lymphoma Prognostic Factors Project. A predictive model for aggressive non-Hodgkin's lymphoma. *N Engl J Med*. 1993;329(14):987-994.
15. Sehn LH, Berry B, Chhanabhai M, et al. The Revised International Prognostic Index (R-IPI) is a better predictor of outcome than the standard IPI for patients with diffuse large B-cell lymphoma treated with R-CHOP. *Blood*. 2007;109(5):1857-1861.
16. Zhou Z, Sehn LH, Rademaker AW, et al. An enhanced International Prognostic Index (NCCN-IPI) for patients with diffuse large B-cell lymphoma treated in the rituximab era. *Blood*. 2014;123(6):837-842.
17. Cheson BD, Pfistner B, Juweid ME, et al. Revised response criteria for malignant lymphoma. *J Clin Oncol*. 2007;25(5):579-586.
18. Juweid ME, Stroobants S, Hoekstra OS, et al. Use of positron emission tomography for response assessment of lymphoma: consensus of the Imaging Subcommittee of International Harmonization Project in Lymphoma. *J Clin Oncol*. 2007;25(5):571-578.
19. Khan AB, Barrington SF, Mikhaeel NG, et al. PET-CT staging of DLBCL accurately identifies and provides new insight into the clinical significance of bone marrow involvement. *Blood*. 2013;122(1):61-67.
20. Barrington SF, Mikhaeel NG, Kostakoglu L, et al. Role of imaging in the staging and response assessment of lymphoma: consensus of the International Conference on Malignant Lymphomas Imaging Working Group. *J Clin Oncol*. 2014;32(27):3048-3058.
21. Cheson BD, Fisher RI, Barrington SF, et al. Recommendations for initial evaluation, staging, and response assessment of Hodgkin and non-Hodgkin lymphoma: the Lugano classification. *J Clin Oncol*. 2014;32(27):3059-3068.
22. Alzahrani M, El-Galaly TC, Hutchings M, et al. The value of routine bone marrow biopsy in patients with diffuse large B-cell lymphoma staged with PET/CT: a Danish-Canadian study. *Ann Oncol*. 2016;27(6):1095-1099.
23. Meignan M, Gallamini A, Meignan M, et al. Report on the first international workshop on interim-PET-scan in lymphoma. *Leuk Lymphoma*. 2009;50(8):1257-1260.
24. Mikhaeel NG, Smith D, Dunn JT, et al. Combination of baseline metabolic tumour volume and early response on PET/CT improves progression-free survival prediction in DLBCL. *Eur J Nucl Med Mol Imag*. 2016;43(7):1209-1219.
25. Meignan M, Cottreau AS, Versari A, et al. Baseline metabolic tumor volume predicts outcome in high-tumor-burden follicular lymphoma: a pooled analysis of three multicenter studies. *J Clin Oncol*. 2016;34(30):3618-3626.
26. Kostakoglu L, Dalmasso F, Berchiolla P, et al. A prognostic model integrating PET-derived metrics and image texture analyses with clinical risk factors from GOYA. *eJHaem*. 2022;3(2):406-414.
27. Schmitz C, Huttman A, Muller SP, et al. Dynamic risk assessment based on positron emission tomography scanning in diffuse large B-cell lymphoma: post-hoc analysis from the PETAL trial. *Eur J Cancer*. 2020;124:25-36.
28. Cottreau AS, Lanic H, Mareschal S, et al. Molecular profile and FDG-PET/CT total metabolic tumor volume improve risk classification at diagnosis for patients with diffuse large B-cell lymphoma. *Clin Cancer Res*. 2016;22(15):3801-3809.
29. Vercellino L, Cottreau AS, Casasnovas O, et al. High total metabolic tumor volume at baseline predicts survival independent of response to therapy. *Blood*. 2020;135(16):1396-1405.
30. Kostakoglu L, Martelli MSLH, Belada D, et al. Baseline PET-derived metabolic tumor volume metrics predict progression-free and overall survival in DLBCL after first-line treatment: results from the phase 3 GOYA study. *Blood*. 2017;130:824.
31. Vitolo U, Trneny M, Belada D, et al. Obinutuzumab or rituximab plus cyclophosphamide, doxorubicin, vincristine, and prednisone in previously untreated diffuse large B-cell lymphoma. *J Clin Oncol*. 2017;35(31):3529-3537.

32. Duhrsen U, Muller S, Hertenstein B, et al. Positron Emission Tomography-Guided Therapy of Aggressive Non-Hodgkin Lymphomas (PETAL): a multicenter, randomized phase III trial. *J Clin Oncol*. 2018;36(20):2024-2034.
33. Meignan M, Sasanelli M, Casasnovas RO, et al. Metabolic tumour volumes measured at staging in lymphoma: methodological evaluation on phantom experiments and patients. *Eur J Nucl Med Mol Imag*. 2014;41(6):1113-1122.
34. Orlhac F, Eertink JJ, Cottreau AS, et al. A guide to ComBat harmonization of imaging biomarkers in multicenter studies. *J Nucl Med*. 2022;63(2):172-179.
35. Kalbfleisch JD, Prentice RL. *The Statistical Analysis of Failure Time Data*. JohnWiley & Sons; 1980.
36. Pencina MJ, D'Agostino RB Sr, Steyerberg EW. Extensions of net reclassification improvement calculations to measure usefulness of new biomarkers. *Stat Med*. 2011;30(1):11-21.
37. Sehn LH, Salles G. Diffuse large B-cell lymphoma. *N Engl J Med*. 2021;384(9):842-858.
38. Pfreundschuh M, Ho AD, Cavallin-Stahl E, et al. Prognostic significance of maximum tumour (bulk) diameter in young patients with good-prognosis diffuse large-B-cell lymphoma treated with CHOP-like chemotherapy with or without rituximab: an exploratory analysis of the MabThera International Trial Group (MInT) study. *Lancet Oncol*. 2008;9(5):435-444.
39. Barrington SF, Meignan M. Time to prepare for risk adaptation in lymphoma by standardizing measurement of metabolic tumor burden. *J Nucl Med*. 2019;60(8):1096-1102.
40. Cottreau AS, Meignan M, Nioche C, et al. Risk stratification in diffuse large B cell lymphoma using lesion dissemination and metabolic tumor burden calculated from baseline PET/CT. *Ann Oncol*. 2021;32(3):404-411.
41. Kurtz DM, Scherer F, Jin MC, et al. Circulating tumor DNA measurements as early outcome predictors in diffuse large B-cell lymphoma. *J Clin Oncol*. 2018;36(28):2845-2853.
42. Cheson BD. Predicting the future for DLBCL. *Blood*. 2020;135(16):1308-1309.